Title

A Tail Fiber Protein and a Receptor-Binding Protein Mediate ICP2 Bacteriophage Interactions with Vibrio cholerae OmpU

Journal

Journal of Bacteriology, 203(13)

ISSN

0021-9193

Authors

Lim, Andrea NW
Yen, Minmin
Seed, Kimberley D
et al.

Publication Date

2021-06-08

DOI

10.1128/jb.00141-21

Peer reviewed

AMERICAN SOCIETY FOR MICROBIOLOGY | Journal of Bacteriology®

RESEARCH ARTICLE

A Tail Fiber Protein and a Receptor-Binding Protein Mediate ICP2 Bacteriophage Interactions with *Vibrio cholerae* OmpU

Andrea N. W. Lim,[a] Minmin Yen,[a]* Kimberley D. Seed,[a]* David W. Lazinski,[a] Andrew Camilli[a,b]

[a]Department of Molecular Biology and Microbiology, Tufts University School of Medicine, Boston, Massachusetts, USA
[b]Department of Molecular Biology and Microbiology, Graduate School of Biomedical Sciences, Tufts University School of Medicine, Boston, Massachusetts, USA

ABSTRACT ICP2 is a virulent bacteriophage (phage) that preys on *Vibrio cholerae*. ICP2 was first isolated from cholera patient stool samples. Some of these stools also contained ICP2-resistant isogenic *V. cholerae* strains harboring missense mutations in the trimeric outer membrane porin protein OmpU, identifying it as the ICP2 receptor. In this study, we identify the ICP2 proteins that mediate interactions with OmpU by selecting for ICP2 host range mutants within infant rabbits infected with a mixture of wild-type and OmpU mutant strains. ICP2 host range mutants that can now infect OmpU mutant strains have missense mutations in the putative tail fiber gene *gp25* and the putative adhesin gene *gp23*. Using site-specific mutagenesis, we show that single or double mutations in *gp25* are sufficient to generate the host range mutant phenotype. However, at least one additional mutation in *gp23* is required for robust plaque formation on specific OmpU mutants. Mutations in *gp23* alone were insufficient to produce a host range mutant phenotype. All ICP2 host range mutants retained the ability to form plaques on wild-type *V. cholerae* cells. The strength of binding of host range mutants to *V. cholerae* correlated with plaque morphology, indicating that the selected mutations in *gp25* and *gp23* restore molecular interactions with the receptor. We propose that ICP2 host range mutants evolve by a two-step process. First, *gp25* mutations are selected for their broad host range, albeit accompanied by low-level phage adsorption. Subsequent selection occurs for *gp23* mutations that further increase productive binding to specific OmpU alleles, allowing for near-wild-type efficiencies of adsorption and subsequent phage multiplication.

IMPORTANCE Concern over multidrug-resistant bacterial pathogens, including *Vibrio cholerae*, has led to renewed interest in phage biology and the potential for phage therapy. ICP2 is a genetically unique virulent phage isolated from cholera patient stool samples. It is also one of three phages in a prophylactic cocktail that have been shown to be effective in animal models of infection and the only one of the three that requires a protein receptor (OmpU). This study identifies an ICP2 tail fiber and a receptor binding protein and examines how ICP2 responds to the selective pressures of phage-resistant OmpU mutants. We found that this particular coevolutionary arms race presents fitness costs to both ICP2 and *V. cholerae*.

KEYWORDS OmpU, tail fiber protein, *Vibrio cholerae*, arms race, bacteriophages

Vibriophages, phages that prey on bacteria of the Gram-negative *Vibrio* genus, were first described by E. H. Hankin as antimicrobial agents from the Ganges River in 1896, 2 decades before phages were formally identified by Twort and d'Hérelle (1, 2). Growing concern over the emergence of multidrug-resistant strains of *Vibrio cholerae* (3), the causative agent of cholera, has renewed scientific interest in vibriophages as therapeutics (2, 4) and environmental markers of cholera outbreaks (5–7). In 2011, our lab isolated three unique virulent vibriophages, designated phages ICP1, ICP2, and ICP3, from the rice-water stools of Bangladeshi cholera patients (7). ICP2 is morphologically categorized as a short-tailed

Citation Lim ANW, Yen M, Seed KD, Lazinski DW, Camilli A. 2021. A tail fiber protein and a receptor-binding protein mediate ICP2 bacteriophage interactions with *Vibrio cholerae* OmpU. J Bacteriol 203:e00141-21. https://doi.org/10.1128/JB.00141-21.

Editor Laurie E. Comstock, Brigham and Women's Hospital/Harvard Medical School

Address correspondence to Andrew Camilli, andrew.camilli@tufts.edu.

* Present address: Minmin Yen, PhagePro, Inc., Boston, Massachusetts, USA; Kimberley D. Seed, Department of Plant and Microbial Biology, University of California, Berkeley, Berkeley, California, USA.

Received 8 March 2021
Accepted 9 April 2021
Accepted manuscript posted online 19 April 2021
Published 8 June 2021

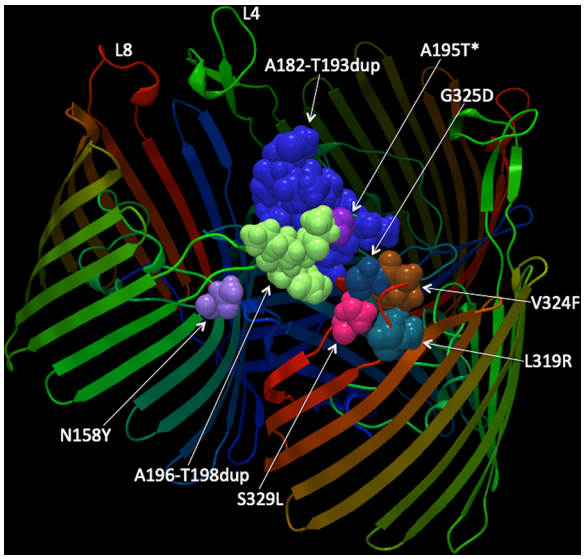

FIG 1 Locations of mutated amino acid residues in the OmpU structure that give rise to ICP2 resistance. OmpU mutations previously shown to confer ICP2 resistance (8) map to extracellular loops L4 and L8 on the structure solved by Li et al. (16). The OmpU porin is a homotrimer of three β-barrels. Mutations are highlighted on two adjacent monomers to emphasize their proximity. *, the A195T mutation confers only partial resistance to ICP2 (8). This image does not show how these mutations may affect OmpU structure.

podovirus but bears little genetic homology to the canonical podovirus T7 or other members of the family. Its 50-kb genome contains 73 putative protein-coding sequences divided into two transcriptional units in opposite orientations.

An isolate of ICP2 was also recovered in 2014 from the rice-water stool of a Haitian cholera patient (8). This sample also contained several ICP2-resistant isogenic *V. cholerae* strains that had missense mutations in *ompU*. OmpU is an outer membrane general porin that is associated with virulence (9–11), adherence (12), and osmoregulation (13–15). ICP2-resistant strains with null mutations in *toxR* were also found among several stool samples containing ICP2. ToxR is a transcriptional activator of virulence genes, including *ompU*. Accordingly, the *toxR* null mutations resulted in attenuated *V. cholerae* colonization in an infant mouse model as well as the complete loss of *ompU* expression (9). Further experiments showed that two OmpU missense mutations, V324F and G325D, only minimally affect *V. cholerae* fitness. These mutations identified OmpU as the ICP2 receptor and demonstrated how vibriophages impose selective pressures during cholera infections.

In 2018, two groups solved the crystal structure of *V. cholerae* OmpU (16, 17). OmpU is an outer-membrane-localized-homotrimer, with each monomer consisting of a 16-β-stranded barrel. Each monomer has a central pore ~0.55 to 0.6 nm wide (17) and has eight protruding extracellular loops (Fig. 1). L2 projects into the neighboring monomer, while L3 is a constriction loop that bends into the center of each barrel. The OmpU residues that mutated to confer ICP2 resistance in the stool samples (8) are highlighted on one monomer-monomer interface in Fig. 1 (8, 16). All mutations, except N158Y, are in L4 or L8. These extracellular loops are adjacent between neighboring monomers. N158Y is found near the transmembrane region of L3, and its effects on OmpU localization or structure are unknown. These observations suggest that ICP2 binds *V. cholerae* at the L4 and L8 interfaces of OmpU trimers. We sought to identify the ICP2 proteins that interact with OmpU and to examine how ICP2 may counterevolve in response to phage-resistant *V. cholerae* OmpU mutants.

RESULTS

ICP2 host range mutants have missense mutations in *gp23* and *gp25*. ICP2 host range mutants were selected during intestinal infection of infant rabbits coinoculated with ICP2 and a mixture of *V. cholerae* wild-type (WT) and OmpU point mutant strains

at a 10:1 ratio. ICP2 host range mutants were defined by their ability to infect OmpU mutant host cells that are resistant to WT ICP2. The host strains used in this study are isogenic aside from their OmpU mutations, and host range refers to this range of *V. cholerae* mutants (Table 1). The addition of WT *V. cholerae* was designed to allow for enough replication of ICP2 to yield spontaneous host range mutants that could then be enriched by replicating on the OmpU mutants. Until the appearance of such host range mutants, the OmpU mutants have a competitive advantage over WT *V. cholerae* due to lack of predation by ICP2. Indeed, this was shown previously when ICP2 predation resulted in a 10,000-fold competitive advantage for OmpU G325D over the WT after 12 h of infection of infant rabbits (8). One group of four animals was inoculated with WT *V. cholerae* and a mixture of OmpU A196_Y198dup, OmpU A195T, OmpU L319R, and OmpU S329L strains. A second group of four animals was inoculated with the WT and a mixture of OmpU A182_T193dup, OmpU V324F, and OmpU N158Y strains. A third group of four animals was infected with WT and OmpU G325D strains. All of the OmpU mutants, except for the OmpU A195T mutant, are resistant to WT ICP2. OmpU A195T is partially resistant to WT phage (8) (Fig. 1). ICP2 host range mutants in cecal fluid obtained from euthanized symptomatic animals were isolated via plaque assays with soft agarose overlays containing specific OmpU mutants. These included the OmpU A195T, V324F, and G325D mutants. OmpU G325D was the more prevalent mutation identified in the Haitian stool sample containing ICP2 and was also found in several Bangladeshi samples. OmpU V324F and A195T were also among the Bangladeshi samples (8); the latter mutant was specifically chosen because it occurs in L4, whereas G325D and V324F occur in L8 of OmpU. As many as seven plaques per host strain per animal were chosen for plaque purification on each respective OmpU mutant. All plaques were clear and equivalent in size to those formed by WT ICP2 on WT *V. cholerae*.

The whole genomes of 13 ICP2 host range mutants were sequenced to identify possible mutations. Of the 13 isolates sequenced, all were unique (Fig. 2A). Those isolated on the OmpU V324F or OmpU G325D mutant contained multiple single nucleotide variants (SNVs) in *gp23* and *gp25* (Fig. 2A), each a missense mutation. This strongly implicates Gp23 and/or Gp25 as an ICP2 protein that interacts with the OmpU receptor. According to homology analysis via Iterative Threading Assembly Refinement (I-TASSER) (18–20) and Rapid Annotation using Subsystem Technology (RAST), version 2 (21, 22), *gp23* encodes a putative receptor binding adhesin protein and *gp25* encodes a putative phage tail fiber. Although *gp24* is also annotated as a putative tail fiber, no mutations were found in this gene. It is unlikely that Gp23 and Gp25 are tail tube proteins, because those have previously been identified bioinformatically as Gp9, Gp10, and Gp11 (23).

ICP2 mutants isolated on the OmpU V324F strain have a Gp23 S188A mutation, while those isolated on the OmpU G325D strain have a Gp23 S209R mutation (Fig. 2A). Gp25 mutations were more prevalent and differed among the ICP2 host range mutants. Gp25 mutations clustered near the N and C termini, which are outside or near the ends of two predicted collagen fiber-like domains (Fig. 2). Gp25 mutations exhibited loose specificity for individual OmpU alleles. Residues Q510 and N690 both mutated to different amino acids in different ICP2 phages isolated on the OmpU G325D mutant. In contrast, a single S742P mutation was shared among phages isolated on both OmpU V324F and G325D mutants. Because these ICP2 host range mutants were selected during intestinal infection, we could not determine how many rounds of phage replication occurred before the phage developed the ability to infect an OmpU mutant or in what order Gp23 and Gp25 mutations were selected. Therefore, we next sought to parse the relationship between the ICP2 Gp23 and Gp25 mutations and *V. cholerae* OmpU alleles.

ICP2 host range mutants require at least one Gp25 mutation. Plasmid-based recombination in *V. cholerae* was used to generate ICP2 mutants with several of the *gp25* mutations identified in host range mutants that evolved *in vivo*. Gp25 S742P was present in two host range mutants isolated on the OmpU V3234F and G325D mutants.

TABLE 1 Bacterial strains, phages, and plasmids

Strain, plasmid, or phage	Description	Source or reference
Strains		
Vibrio cholerae		
WT	O1 El Tor Ogawa E7946 (Sm^r)	39
AC2846	E7946 Δ*ompU*	40
AC6034	E7946 ΔK139 prophage	Lab collection
KS714	E7946 Δ*lacZ*::Kan^r OmpU A182_T193dup	This study
KS769	E7946 Δ*lacZ*::Kan^r OmpU V324F	This study
KS784	E7946 Δ*lacZ*::Kan^r OmpU A196_Y198dup	This study
KS785	E7946 Δ*lacZ*::Spec^r OmpU A195T	This study
KS823	E7946 Δ*lacZ*::Spec^r OmpU L319R	8
KS824	E7946 Δ*lacZ*::Spec^r OmpU S329L	8
KS825	E7946 Δ*lacZ*::Spec^r OmpU N158Y	8
KS745	E7946 OmpU G325D	8
KS667	E7946 OmpU A196_Y198dup	8
KS658	E7946 OmpU A195T	8
KS672	E7946 OmpU V324F	8
KS822	E7946 OmpU A182_T193dup Δ*lacZ*::Spec^r	8
AC4653	E7469 Δ*wbeL* (Sm^r)	41
AC5218	E7469 Δ*mutS*::*aad9* (Sm^r Sp^r)	24
AC6727	E7946 Δ*wbeL* ΔK139-*att*::*aph* Δ*mutS*::*aad9* (Sm^r Km^r Sp^r)	This study
E. coli		
AC5981	TG1	Lab collection
AC89	Sm10(λpir)	Lab collection
Plasmids		
pDL1201	Plasmid backbone for recombination (Amp^r)	Lab collection
pDL1201_gp23-Kan-25	pDL1201_*gp23-neo-gp25*	This study
pDL1201_23_GD(6)	pDL1201_*gp23*(209R)-*neo-gp25*	This study
pDL1201_23_VF(2)	pDL1201_*gp23*(S188A)-*neo-gp25*	This study
pDL1201_25_GD(1)	pDL1201_*gp23-neo-gp25*(D96N S676A)	This study
pDL1201_25_GD(6)	pDL1201_*gp23-neo-gp25*(K159E S742P)	This study
pDL1201_25_VF(2)	pDL1201_*gp23-neo-gp25*(S742P)	This study
Phage ICP2	ICP2_2013_A_Haiti[a]	8

[a]GenBank accession no. NC_024791.1.

The mutant isolated on *V. cholerae* OmpU G325D also contained a unique second mutation, K159E. A phage mutant isolated on the OmpU G325D strain also contained Gp25 D96N and S676A mutations (Fig. 2A). Recombinant phages with single Gp25 S742P mutations were isolated, plaque-purified once on the OmpU V324F strain, and then amplified on the WT strain. Recombinants with Gp25 D96N and S676A mutations were isolated, plaque purified once on the OmpU G325D strain, and then amplified on the WT strain. We chose to amplify on the WT strain instead of an OmpU mutant in order to limit further selection for spontaneous mutations that might increase infectivity on the latter host. All host range mutants isolated in this study formed clear, normal-size plaques on the WT strain, suggesting that there would not be selective pressure for additional mutations on this host. Control recombination infections using a plasmid containing WT *gp23* and *gp25* did not result in any host range mutants. Recombinant mutants are shown in Fig. 2C.

Efficiency-of-plating (EOP) assays were used to quantify how efficiently these mutants can infect OmpU V324F and G325D cells relative to WT cells. Low EOPs often correlated with a turbid plaque morphology (representative images of plaque morphologies are shown in Fig. 3A). Recombinant ICP2 mutants with only one or two Gp25 mutations maintain the ability to form clear plaques on WT host cells but can only weakly form plaques (i.e., low EOPs and turbid plaques) on the OmpU V324F or OmpU G325D mutant. No host range mutants formed plaques on a Δ*ompU* control, indicating that they are interacting with either OmpU V324F or OmpU G325D and not with another receptor. A recombinant phage with a single Gp25 S742P mutation forms

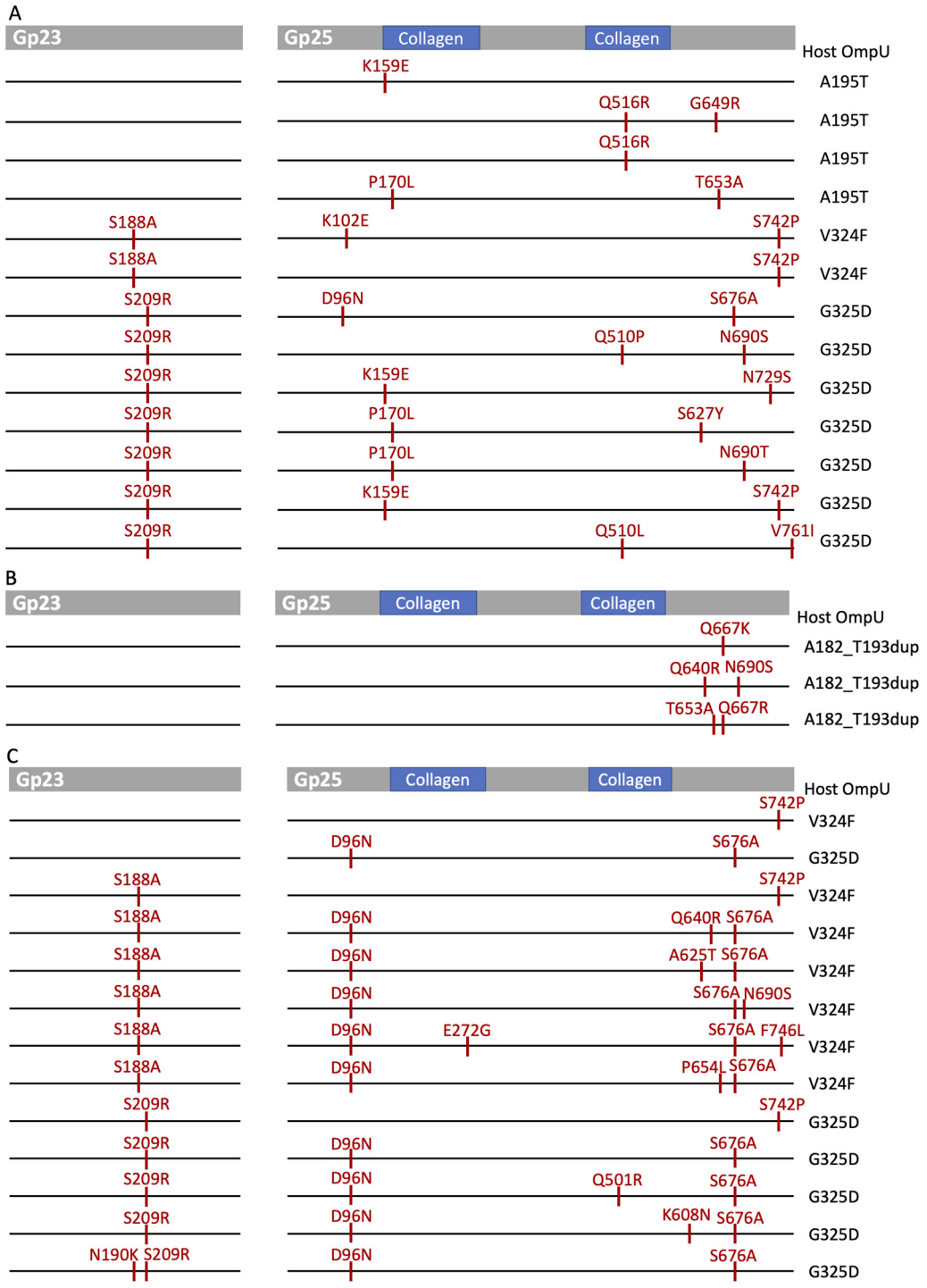

FIG 2 ICP2 host range mutants have missense mutations in *gp23* and *gp25*. Thick gray bars represent the WT amino acid sequences of Gp23 and Gp25, with putative domains indicated where possible. Each pair of thin horizontal lines represents the Gp23 and Gp25 proteins of a single ICP2 mutant. The mutations present in each isolate are shown above the corresponding red tick marks. The OmpU allele of the host on which each phage mutant was isolated is indicated on the right. (A) ICP2 host range mutants isolated from the cecal fluid of coinfected infant rabbits had mutations in *gp23* and *gp25*. (B) ICP2 host range mutants selected *in vitro* on the OmpU A182_T193dup mutant had mutations in *gp25*. (C) Recombinant ICP2 host range mutants were generated *in vitro* through sequential infections of WT *V. cholerae* strains carrying plasmids with specific *gp23* or *gp25* mutations. Mutants were selected based on their abilities to form plaques on either the OmpU V324F or the OmpU G325D strain. Several isolates acquired one or two novel mutations during the second recombination infection.

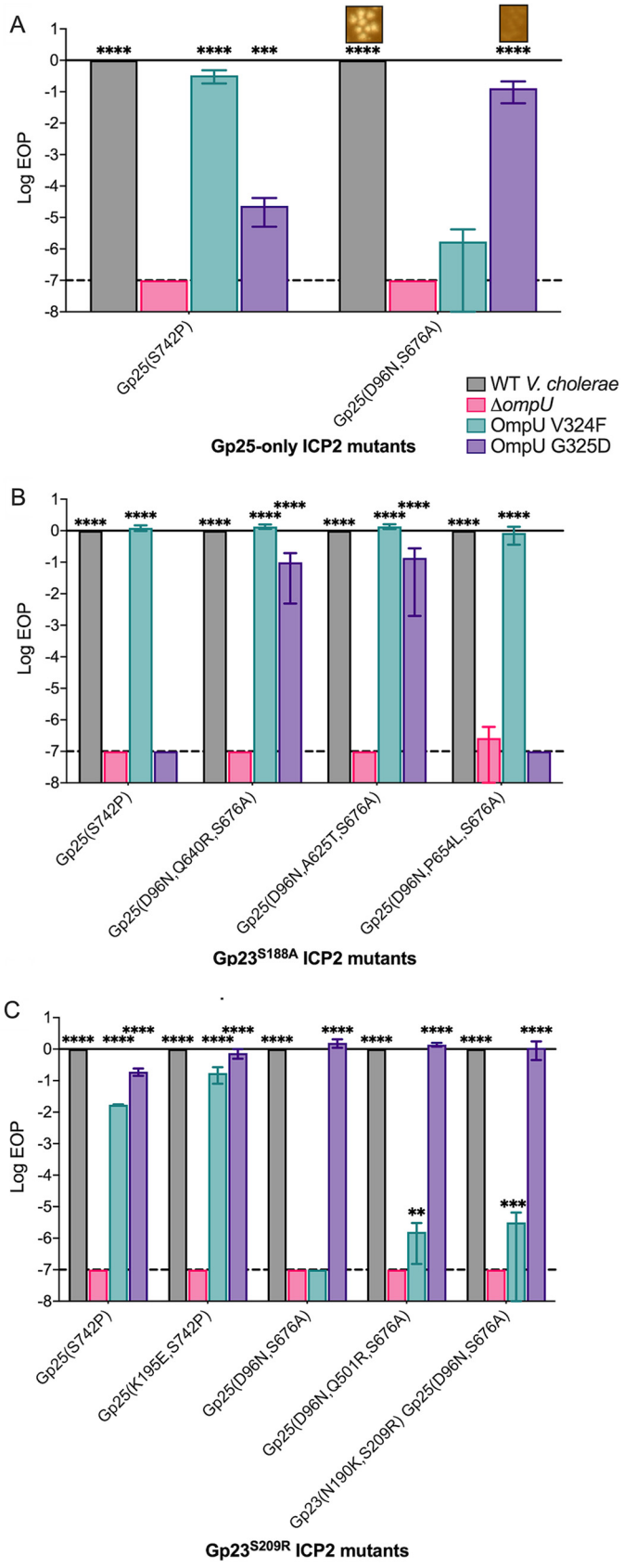

FIG 3 Efficiencies of plating of ICP2 host range mutants on the OmpU V324F and G325D strains. EOPs were determined relative to that on WT *V. cholerae*. EOP assays were carried out in at least

(Continued on next page)

turbid plaques on both the OmpU V324F and G325D mutants, but its EOP on the OmpU V324F mutant is only 10-fold lower than that on the WT (Fig. 3A). In contrast, its EOP on the OmpU G325D mutant is 4 to 5 log units lower than that on the WT. A recombinant ICP2 mutant with Gp25 mutations D96N and S676A also forms turbid plaques on both the OmpU V324F and G325D strains. It has a clear preference for the OmpU G325D strain, barely reaching a statistically significant EOP on the OmpU V324F strain. While Gp25 mutations alone do not provide robust phenotypes, at least one is required to weakly infect an OmpU mutant.

Further support for the important role of Gp25 in conferring a host range phenotype came from host range mutants that evolved in animals and were then isolated on *V. cholerae* OmpU A195T, a host strain only partially resistant to WT ICP2 (8). These phage mutants have one or two mutations in Gp25 and no mutations in Gp23 (Fig. 2A). This provides further evidence that Gp25 mutations are sufficient to expand the host range.

In host range assays that included five additional ICP2-resistant OmpU mutants, ICP2 mutants with only one or two Gp25 mutations and no Gp23 mutations exhibited similar host range patterns despite the diversity of their Gp25 mutations (Fig. 4, top nine ICP2 mutants). In addition to forming clear plaques on WT *V. cholerae*, most of these host range mutants had higher EOPs than WT ICP2 on the OmpU L319R, S329L, and A182_T193dup mutants. This suggests that initial Gp25 mutations are necessary and sufficient to expand host range.

Selection of ICP2 host range mutants *in vitro*. The observation that all ICP2 host range mutants isolated in animals retain the ability to form plaques on WT *V. cholerae* could be due to fact that both WT *V. cholerae* and OmpU mutants were present during the selection. To investigate this hypothesis, we sought to isolate host range mutants *in vitro* on pure cultures of the OmpU A182_T193dup strain and then to test plaque formation on WT *V. cholerae*. Initial attempts to select ICP2 host range mutants *in vitro* failed, likely due to the lack of a pool of input phage that was large enough to harbor preexisting mutants. To overcome this limitation, we generated two independent high-titer stocks of ICP2 on a mutator strain of *V. cholerae* in which the mismatch repair gene *mutS* was deleted. Deletion of *mutS* has previously been shown to increase the mutation rate of *V. cholerae* by 100-fold (24). Although it is not known if the host methyl-directed mismatch repair system functions with ICP1 DNA replication, it is notable that ICP1 encodes its own DNA adenine methyltransferase (Dam) (8). After two rounds of selection on the OmpU A182_T193dup strain, host range mutants that formed clear plaques were obtained. Whole-genome sequencing of four ICP2 host range mutants from each independent selection yielded a total of four lineages: one from the first and three from the second selection. Previously observed and novel mutations in *gp25* were found, but no mutations were present in *gp23* (Fig. 2B). Two mutants contained the previously observed single Gp25 S742P mutation. Only the three host range mutants with novel Gp25 mutations are shown in Fig. 2B and were further analyzed. These results are consistent with those obtained from the *in vivo*-selected host range mutants in that mutations in Gp25 are sufficient to give a host range phenotype on an OmpU A182_T193dup strain.

FIG 3 Legend (Continued)
quadruplicate with a starting titer of $\sim 10^8$ PFU/ml. Dashed lines represent the limit of detection; bars show means; error bars represent standard deviations. No data points were included for plaques that were too turbid to count. Examples of plaque morphology are shown above their associated bars. Plaque assays were scanned using Epson Scan (version 3.25A), with adjustments made to contrast and histogram input and output in order to best visualize turbid plaques. Scanner settings were kept the same for all plates in a single replicate. Statistical significance was determined relative to the absence of plaque formation on the Δ*ompU* mutant (by ordinary one-way analysis of variance and a *post hoc* Dunnett's multiple-comparison test on log-transformed data points). *, $P \leq 0.05$; **, $P \leq 0.01$; ***, $P \leq 0.001$; ****, $P \leq 0.0001$. (A) Recombinant ICP2 mutants with only one or two Gp25 mutations have lower EOPs and form turbid plaques on *V. cholerae* OmpU V324F or OmpU G325D. They also retain the ability to form clear plaques on WT cells. (B) ICP2 host range mutants with secondary Gp23 S188A mutations form clear plaques on the OmpU V324F strain and have EOPs near 1, regardless of their Gp25 mutations. Several recombinant isolates also retain the ability to weakly infect the OmpU G325D strain. (C) ICP2 host range mutants with secondary Gp23 S209R mutations have increased EOPs on the OmpU G325D strain, regardless of their Gp25 mutations.

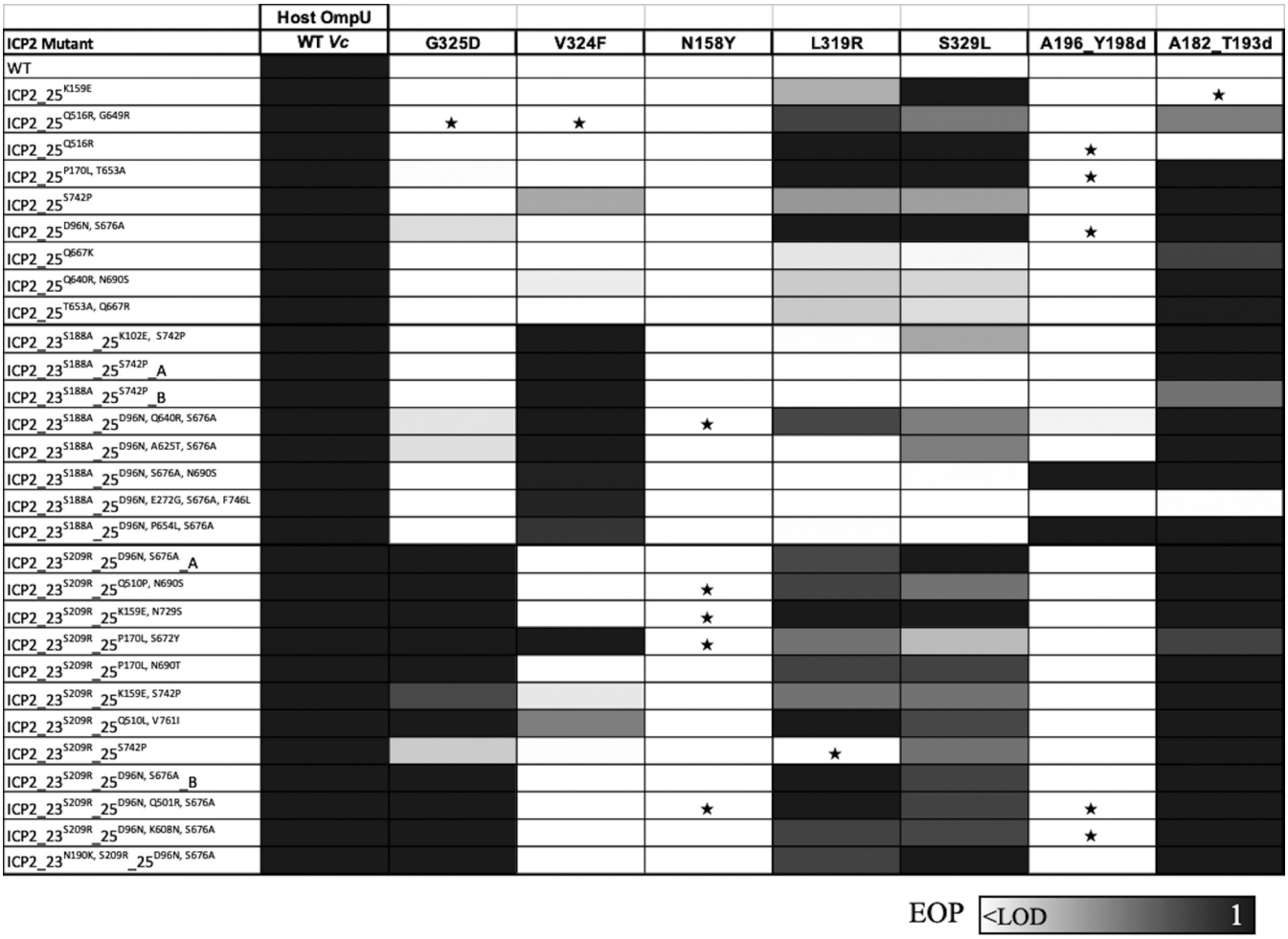

FIG 4 Host range efficiency-of-plating assays on ICP2-resistant OmpU mutants. Host range mutants are organized in rows from top to bottom according to their Gp23 mutations: the top 10 have no Gp23 mutations; the middle 8 have Gp23 S188A; the bottom 12 have Gp23 S209R. The bottom mutant also has a second Gp23 mutation, N190K. Approximate EOPs from below the limit of detection (<LOD) to 1, indicated by the scale bar below the chart, are based on the means for two to five replicates; averages of >1 were set to 1. The ICP2 mutants for which log EOPs are shown in Fig. 3 were not retested on the OmpU V324F and OmpU G325D strains; these boxes use the mean EOP values from Fig. 3. A star indicates that lysis at lower dilutions was observed in at least two replicates, without single plaques at higher dilutions. Mutants followed by capital letters (A, B, or C) are from sets of biological replicates (see Table S2 in the supplemental material). ICP2 $Gp23^{188A}Gp25^{S742P}$_A evolved *in vivo*, while ICP2 $Gp23^{188A}Gp25^{S742P}$_B is a recombinant phage. Similarly $Gp23^{S209R}Gp25^{D96N,\ S676A}$_A evolved *in vivo*, and $Gp23^{S209R}Gp25^{D96N,\ S676A}$_B is a recombinant phage.

Next, we compared EOPs and plaque phenotypes on the OmpU A182_T193dup strain and WT *V. cholerae*. The three host range mutants formed clear plaques on the OmpU A182_T193dup strain, and, as observed for the *in vivo*-selected host range mutants, all retained clear plaque formation on WT *V. cholerae* (Fig. 4, 8th to 10th rows). In agreement with this, their EOPs on OmpU A182_T193dup and the WT were at or near 1. These mutants formed turbid plaques on *V. cholerae* OmpU L319R and S329L, like the other Gp25-only mutants. Therefore, retention of infection of WT *V. cholerae* in ICP2 host range mutants appears to be a general phenomenon and not the result of selection in the presence of the WT and an OmpU mutant.

Secondary Gp23 mutations increase the EOP on specific OmpU mutants. In an effort to isolate ICP2 host range mutants with only Gp23 mutations, WT *V. cholerae* with plasmids containing *gp23* S188A or S209R alleles were infected with WT ICP2. However, no recombinant plaques could be isolated on the OmpU V324F or G325D strain. When the population of progeny phages from these infections was sequenced, ~1% of the phage were found to have the intended mutations. Therefore, it appears that Gp23 mutations alone are insufficient to give a host range phenotype.

A secondary Gp23 S188A mutation in Gp25-only mutants imparted clear plaque formation on the OmpU V324F strain. Host range mutants with secondary Gp23 mutations were generated by using the ICP2 recombinants with one or two Gp25 mutations to infect WT cells harboring plasmids containing either the *gp23* S188A or the *gp23* S209R allele. The addition of Gp23 S188A led to more-efficient plaque formation on the OmpU V324F strain for all seven recombinants, regardless of initial Gp25 mutations (Fig. 3B). This still held true when recombinant phages gained additional novel Gp25 mutations during the second recombination infection, as in the last three samples for which log EOPs are shown in Fig. 3B.

Similarly, a secondary Gp23 S209R mutation resulted in increased EOPs and/or clear-plaque formation for all five recombinants on the OmpU G325D strain regardless of initial Gp25 mutations (Fig. 3C). A phage containing Gp23 S209R and Gp25 S742P was the only recombinant that still formed turbid plaques on the OmpU G325D strain, but its EOP of 0.19 was markedly higher than that of an isolate with a single Gp25 S742P mutation (mean EOP, 2.3×10^{-5}). The addition of a Gp25 K159E mutation increased the EOP further and gave clear plaques on the OmpU G325D strain. The presence of Gp25 S742P also likely allowed for the turbid-plaque formation and low EOPs on the OmpU V324F strain for two of the ICP2 mutants. As with Gp23 S188A secondary mutations, new Gp25 mutations did not result in EOPs on the OmpU V324F and G325D strains that greatly exceeded 1 (Fig. 3C). These results suggest that Gp23 mutations increase infection in a mostly allele-specific manner with respect to OmpU mutants while retaining wild-type infection of WT OmpU.

In EOP assays that included five additional OmpU mutants, ICP2 mutants with secondary Gp23 mutations had modest alterations in host range (Fig. 4). The middle 8 rows in Fig. 4 show the host range of mutants with a secondary Gp23 S188A mutation, and the mutants in the bottom 12 rows all have a secondary Gp23 S209R mutation. The addition of Gp23 S188A corresponded with an inability to form plaques on the OmpU L319R and S329L strains for several ICP2 mutants. In contrast, ICP2 mutants with Gp23 S209R mutations maintained a wider host range that included the OmpU L319R and S329L strains. Additional Gp25 missense mutations that were gained during the sequential recombination process may have also played a role in the host ranges of the remaining ICP2 mutants.

ICP2 host range mutants can bind to OmpU mutants. If plaque formation on the OmpU V324F and G325D mutants requires direct binding by Gp23 and/or Gp25, binding to *V. cholerae* cells with these OmpU alleles should correlate with the EOP. We assayed binding to heat-killed host cells over a period of 24 h and quantified binding as the ratio of the titer of remaining free phage to the initial titer at 0 h. Cells were heat killed by incubation at 51°C for 12 min in a PCR thermocycler. The structure of the cells was unaffected by this treatment as determined by phase-contrast microscopy. WT ICP2 bound to WT *V. cholerae* between 10- and 100-fold, depending on the experiment, but did not exhibit any OmpU-independent binding to the Δ*ompU* strain. All ICP2 host range mutants retained the ability to bind WT *V. cholerae* significantly (Fig. 5).

ICP2 mutants without Gp23 mutations showed no binding to OmpU V324F or G325D cells (Fig. 5A). The fact that these phage mutants could form turbid plaques and had low to intermediate EOPs on these hosts suggests that the binding assay is not very sensitive. All ICP2 mutants with a Gp23 S188A mutation (Fig. 5B) bound to OmpU V324F cells, as expected, considering that these phage mutants have high EOPs and form clear plaques. Similarly, ICP2 mutants with a secondary Gp23 S209R mutation bound to OmpU G325D cells (Fig. 5C). We found one exception to this trend (Fig. 5B). An ICP2_23^{S188A}_25D$^{96N,\ P654L,\ S676A}$ mutant bound to cells with both OmpU alleles, with a preference for OmpU V324F cells, despite not forming plaques or having a detectable EOP on OmpU G325D cells (Fig. 3B).

In general, the host range mutants bound better to WT cells than to OmpU V324F and G325D mutant cells. ICP2_23^{S188A}_25^{S742P} and ICP2_23^{S209R}25^{S742P} showed 99%

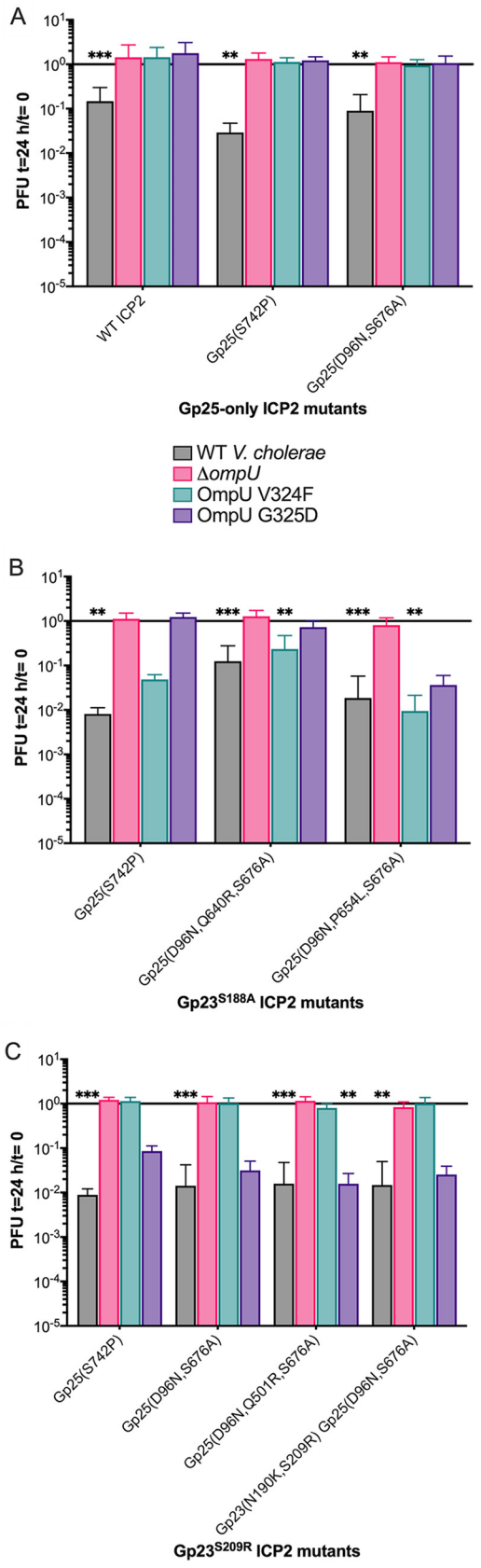

FIG 5 Phage binding to heat-killed OmpU mutant cells. Phage were added to heat-killed cells at an MOI of ~0.1 and were incubated for 24 h at room temperature. Binding was determined as the ratio

(Continued on next page)

binding to WT *V. cholerae* cells but 95% and 91% binding to OmpU V324F and G325D cells, respectively (Fig. 5B and C). Host range mutants with significant binding to OmpU V324F or G325D cells had additional Gp25 mutations (Fig. 5B and C). The additional Gp23 mutation in one Gp23 209R isolate (Fig. 5C) did not significantly aid binding to OmpU G325D cells.

ICP2 host range mutants prey on OmpU mutants in broth culture with various efficiencies. The binding assays demonstrated that phage predation in broth culture differs from the slower diffusion of soft-agar overlays in that the on-off rate of receptor binding will have a larger impact on the rate of adsorption. Therefore, we conducted predation assays in shaking broth cultures to examine how the ICP2 phenotypes seen in EOP and binding assays are reflected in host cell killing. The cell density of early-exponential-growth-phase *V. cholerae* cultures infected with ICP2 host range mutants (multiplicity of infection [MOI], ~1) was measured as the optical density at 600 nm (OD_{600}) over 16 h at 37°C. As reported previously (8), the negative-control Δ*ompU* strain has a slight growth defect in LB medium (Fig. 6A). All ICP2 host range mutants preyed on WT cells, suppressing exponential growth for ~6 h, followed by a return to exponential growth (Fig. 6). Most *V. cholerae* cells replicating after 6 h had gained phage resistance (see Table S1 in the supplemental material).

ICP2 mutants without Gp23 mutations did not affect the growth of the OmpU V324F or OmpU G325D strain (Fig. 6A), correlating with their lack of binding as shown in Fig. 5A. These host range mutants did, however, form turbid plaques and had measurable EOPs on these hosts, presumably due to the slower diffusion of host cells in plaque assays, which allows even weakly binding phages to eventually infect cells.

ICP2 recombinants with secondary Gp23 mutations specifically preyed on either the OmpU V324F or OmpU G325D mutant but not both. Correlating with the intermediate levels of binding in Fig. 5, secondary Gp23 mutations had moderate effects on OmpU V324F or OmpU G325D strain replication (Fig. 6B and C). No host range mutants tested were able to kill both the OmpU V324F and G325D strains. All phage mutants with a secondary Gp23 S188A mutation blocked the OmpU V324F strain in the late-exponential phase. ICP2_23^{S188A}_25$^{D96N,\ Q640R,\ S676A}$ and ICP2_23^{S188A}_25$^{D96N,\ P654L,\ S676A}$ did not disrupt OmpU G325D strain growth, in agreement with their low EOPs (Fig. 3B) and weak binding (Fig. 5B) on this host.

All ICP2 mutations with a secondary Gp23 S209R mutation, except for ICP2_23^{S209R}_25^{S247P}, similarly blocked the OmpU G325D strain in the late-exponential phase. ICP2_23^{S209R}_25$^{D96N,\ Q501R,\ S676A}$ and ICP2_23^{S209R}_25$^{D96N,\ K608N,\ S676A}$ infections led to a much greater delay than ICP2_23^{S209R}_25$^{D96N,\ S676A}$, even though all three phages had significant EOPs on the OmpU G325D strain (Fig. 3C and 6C). ICP2_23^{S209R}_25^{S247P} had no impact on OmpU G325D strain growth, correlating with its turbid plaque morphology and reduced EOP (Fig. 5C).

DISCUSSION

A model of ICP2 evolution within humans. During *V. cholerae* infection in people, the presence of phage ICP2 in the intestinal tract imposes selective pressure, resulting in the appearance of phage escape mutants with mutations in the OmpU receptor. In this scenario, we hypothesize that ICP2 *gp25* mutations are initially selected for

FIG 5 Legend (Continued)
of the PFU remaining at 24 h to the PFU added at 0 h; a ratio near 1 indicates no detectable binding. Each bar represents the mean for 4 to 12 biological replicates (12 replicates for WT ICP2; most samples have 6 to 9 biological replicates). Error bars represent standard deviations. Statistical significance was determined relative to the lack of binding to Δ*ompU* cells (by Kruskal-Wallis and *post hoc* Dunn's multiple-comparison tests). *, $P \leq 0.05$; **, $P \leq 0.01$; ***, $P \leq 0.001$; ****, $P \leq 0.0001$. (A) WT ICP2 binds only to heat-killed WT *V. cholerae* cells. Binding to OmpU V324F or G325D cells by ICP2 mutants with only Gp25 mutations is below the limit of detection of this assay. (B) ICP2 mutants with a secondary Gp23 S188A mutation bind WT and OmpU V324F cells. An ICP2 mutant with an additional new Gp25 P654L mutation also shows some binding to OmpU G325D cells but maintains a preference for OmpU V324F cells. (C) All ICP2 mutants with a secondary Gp23 S209R mutation bind WT and OmpU G325D host cells. None of the phage mutants tested show binding to OmpU V324F cells.

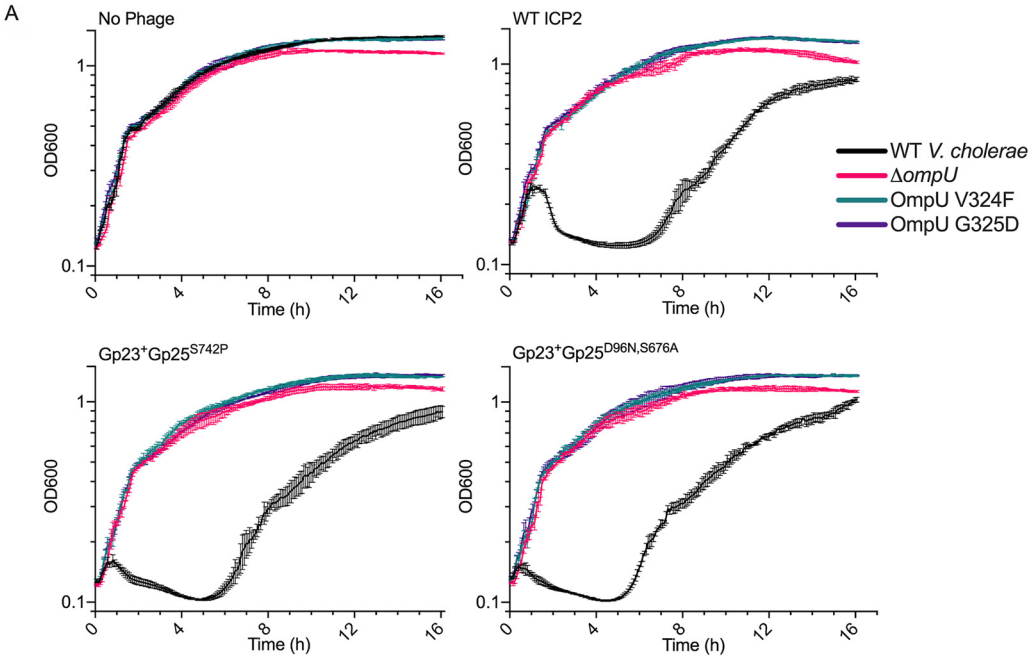

FIG 6 Phage predation killing assays in broth culture. Killing assays were used to evaluate how different ICP2 mutants prey on actively replicating cultures of WT *V. cholerae* and the Δ*ompU*, OmpU V324F, and OmpU G325D mutants. Early- to mid-exponential-growth-phase cells were infected at an MOI of ~1. The optical density at 600 nm was measured every 5 min for 16 h at 37°C in a BioTek plate reader. Each graph represents the mean for three technical replicates. Error bars represent standard deviations. A no-phage control shows that the Δ*ompU* mutant has a slight growth defect. (A) WT ICP2 can prey only on WT *V. cholerae*. ICP2 host range mutants with only Gp25 mutations do not effectively kill *V. cholerae* OmpU V324F or OmpU G325D. (B) ICP2 host range mutants with a secondary Gp23 S188A mutation kill OmpU V324F cells with various degrees of efficiency. (C) ICP2_23^{S209R}_25^{S247P} does not kill OmpU G325D cells despite having a secondary Gp23 S209R mutation, a finding corresponding to its lower EOP and turbid plaque morphology on this host. The remaining ICP2 host range mutants with Gp23 S209R prey on OmpU G325D cells, but with various degrees of efficiency.

increased generalized binding to several OmpU mutants. This generalized binding allows for minimal infection of some OmpU mutant hosts, expanding these phage mutants in the population. Further selection for secondary *gp23* mutations allows for more-efficient infection of hosts with specific OmpU alleles but comes with the risk of a limited host range. For example, phages with Gp23 S188A mutations have a narrow host range, and only five of these nine mutants gained an appreciable ability to form plaques with one to two additional OmpU alleles. Phages with Gp23 S209R mutations have a wider host range: 10 of 12 mutants gained the ability to form plaques with three or four additional OmpU alleles.

V. cholerae forces ICP2 to generate a variety of *gp25* and *gp23* mutations while tempering fitness costs to itself by maintaining a population of functional OmpU alleles (8). This model parallels that described by De Sordi et al. (25) in which phages infect "intermediate" hosts in the microbiome while evolving toward an expanded host range. Initial ICP2 host range mutants with *gp25* mutations are in the process of "jumping" between different OmpU alleles as intermediate hosts. Further studies need to be done to determine if this selective process involves infection processes downstream of OmpU binding, such as DNA injection or virion assembly.

A model of ICP2 tail fiber structure. Speculation on ICP2 tail fiber structure can be made based on the stepwise evolution of Gp25 and Gp23 and on current literature on phage tail fibers and receptor binding proteins (RBPs). Although morphologically in the *Podoviridae* family (7), ICP2 Gp23, Gp24, and Gp25 show surprising similarity to T-even tail fibers in the *Myoviridae* family. Gp25 contains putative collagen-like domains that likely form a triple helical structure, as seen in many other phage tail fibers (26, 27). Gp25 also has a tail tube attachment domain with homology to those of several other podoviruses (23). Homology analysis via Phyre2 (28) and Hardies et al. (23) revealed that Gp24 has regions very similar to P5 of T4 Gp34 and T4 Gp36 (29). Gp34 P5 is one domain of the T4 long tail fiber closest to the phage baseplate. T4 Gp35 and

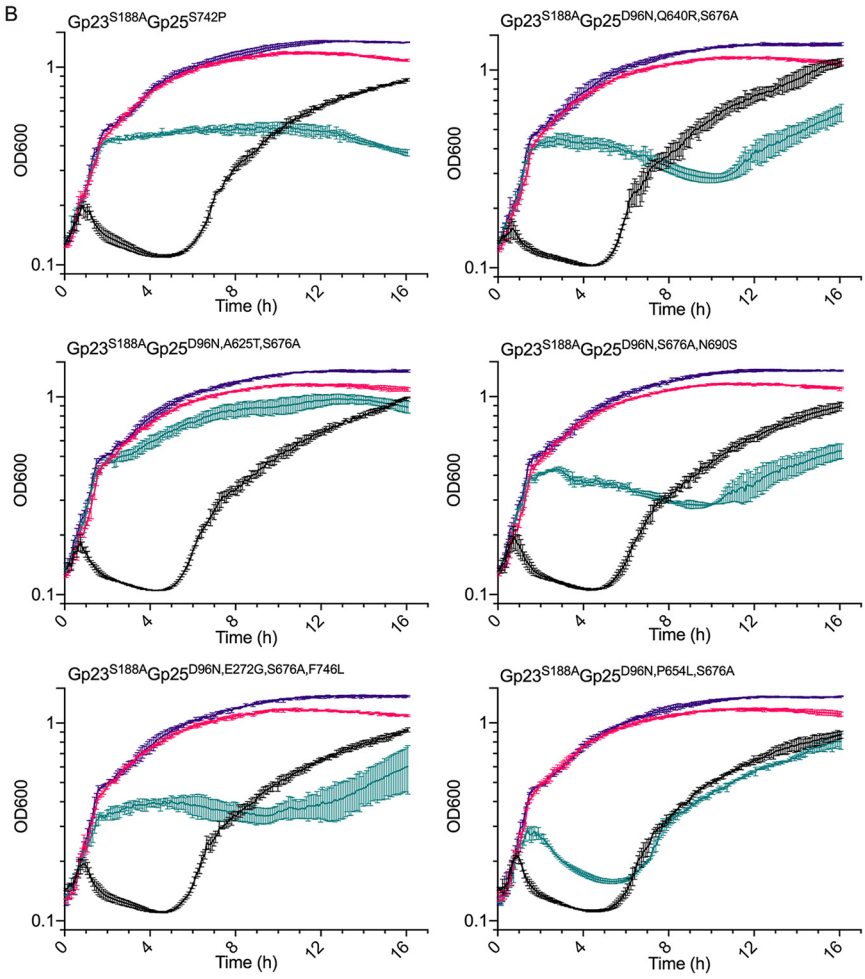

FIG 6 (Continued).

Gp36 make up the "knee" of the T4 long tail fiber (29). None of our ICP2 host range mutants have Gp24 mutations. Gp23 has both structural (23) and functional homology to T-even adhesins that modulate receptor specificity, such as S16 Gp38 and T4 Gp37 and Gp38 (29–31), suggesting that it is the RBP for ICP2.

We hypothesize that *gp25* encodes the long portion of the tail fiber attached to the ICP2 tail tube. Gp25 host range mutations possibly allow for more-permissive receptor binding by Gp23 by altering tail fiber conformation and therefore adsorption. Furthermore, Gp25 and Gp23 may interact with independent portions of OmpU or receptors, one of which must be OmpU, altogether. Gp24 makes up the lower long "shin" of a tail fiber and is then distally bound by Gp23, which lies at the tip of each tail fiber. Biochemical and structural studies will be needed to verify this ICP2 tail fiber model. ICP2 Gp14 also has tail fiber homology (23), and we often find missense mutations in this gene, but without selective pressures other than maintaining viability during storage at 4°C (Table S1). Gp14 mutations do not impact Gp23 and Gp25 interactions with OmpU.

Application. We have yet to find a secondary receptor for ICP2, and the experiments in this study show that ICP2 is dependent on OmpU as its primary receptor. OmpU is a key *V. cholerae* virulence factor (8, 32), limiting its ability to mutate without fitness costs. Our lab has shown previously that a phage cocktail containing ICP1, ICP2, and ICP3 can be used as prophylaxis in two animal models of *V. cholerae* infection (33). In this therapeutic context, these arms race limitations help ensure both the specificity and the efficacy of ICP2.

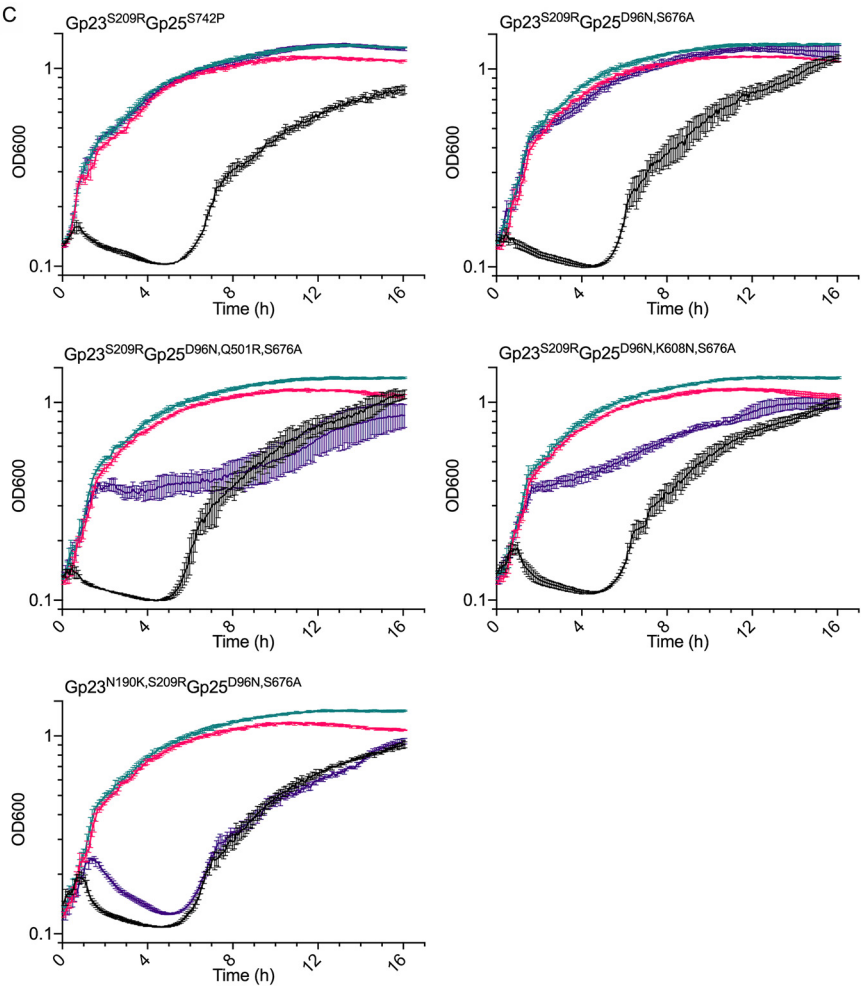

FIG 6 (Continued).

MATERIALS AND METHODS

Strain construction. A mutator strain of *V. cholerae*, designated AC6727 (Table 1), was constructed by moving marked deletions of *mutS* and the K139 prophage into the rough mutant, AC4653, by natural transformation (34). Genomic DNA was purified from strain AC5218 and transformed into AC4653 with selection for spectinomycin resistance (Sp^r). Next, a K139-*att* marked deletion was constructed using splicing-by-overlap-extension (SOE) PCR (2) and transformed into the *wbeL mutS* double mutant with selection for kanamycin resistance (Km^r). The SOE PCR primers (listed 5′ to 3′) used were as follows: CCATATAAACAACCTAGCTTCGGC, GCTAATACAACATTGAGCCTTGGTG, GGTTCTCTCGCGTTTTACCCCCACC TTTATC, GGGTAAAACGCGAGAGAACCGGGGCTATTTG, CCAGGCTTTACACTTTATGCTTCC, CCCGTCCTAAAA CAATTCATCCAG, GGAAGCATAAAGTGTAAAGCCTGGGCGTTTTACCCCCACCTTTATC, and CTGGATGAATTG TTTTAGGACGGGGAGAGAACCGGGGCTATTTG. Strains, phages, and plasmids are listed in Table 1.

Bacteriophage isolation and propagation. ICP2_2013_A_Haiti (referred to here as ICP2) and derivatives were propagated on early-exponential-growth-phase wild-type (WT) *V. cholerae* E7946 (35) growing in Luria-Bertani Miller (LB) broth supplemented with streptomycin (100 μg/ml) at 37°C with aeration. After 3 to 4 h, the lysates were centrifuged at 7,197 $\times$ *g* for 5 min at room temperature (RT) to pellet remaining cells and debris. The supernatants were filtered through 0.22-μm filters and stored as high-titer stocks at 4°C. Stocks were passaged via liquid culture no more than three times to prevent the selection and accumulation of possible mutants. The whole genomes of ICP2 stocks were also regularly sequenced for authentication.

Titers of bacteriophage stocks were determined by plaque assays on WT *V. cholerae* within 3 weeks of use in experiments. Portions (10 μl) of 10-fold serial dilutions of each stock were spotted onto LB–0.3% soft agarose overlays containing approximately 5×10^7 CFU of WT cells and were then dribbled across by tilting the plate. Plates were incubated at 37°C overnight (12 to 18 h).

Genetic analysis of phage isolates. Phage genomic DNA (gDNA) was isolated from high-titer phage stocks by first pretreating with DNase I and RNase A to hydrolyze contaminating host DNA and RNA. Bacteriophage gDNA was then isolated via phenol-chloroform extraction or by use of the DNeasy blood and tissue kit (Qiagen) according to the kit instructions, including the optional proteinase K treatment.

DNA samples were prepared for sequencing on an Illumina HiSeq 2500 system using the Nextera XT kit (Illumina). CLC Genomic Workbench (version 20; Qiagen) was used to map the resulting reads to the ICP2_2013_A_Haiti genome (GenBank accession no. NC_024791.1), and mutations were detected using basic variant detection (see Table S2 in the supplemental material).

Selection of ICP2 host range mutants during intestinal infection. All animal experiments were carried out in accordance with the rules of the Comparative Medicine Services at Tufts University and the Institutional Animal Care and Use Committee. Three-day-old infant rabbits were pretreated with cimetidine HCl (Morton Grove Pharmaceuticals) 3 h prior to infection (36) and were orally inoculated with 5×10^8 CFU of *V. cholerae* in 2.5% sodium bicarbonate (pH 9). A 10:1 mixture of the WT to the OmpU mutant was used. A total of 5×10^6 PFU of ICP2 was added to the bacteria immediately before inoculation to limit phage adsorption *ex vivo*. Rabbits were euthanized 12 h postinoculation, and cecal fluid was collected by dissection and puncture.

Selection of ICP host range mutants *in vitro*. A mutagenized pool of ICP2 was generated by preparing two independent high-titer stocks on the *V. cholerae* mutator strain AC6727. Selection was performed on each ICP2 stock by adding 10^{10} PFU to a 1-liter, mid-exponential phase, 37°C LB broth culture of *V. cholerae* OmpU A182_T193dup. Infection was allowed to proceed overnight. Free phage were purified from the culture supernatant by polyethylene glycol (PEG) precipitation. A second, identical selection was performed using the pool of phage purified from each first-round selection. Host range mutants were screened for by plaque assay on the OmpU A182_T193dup mutant. Clear-plaque mutants were isolated after each of the second selections but not from either first selection. Four phages from each independent selection were plaque-purified on the OmpU A182_T193dup strain.

Homologous recombination of ICP2 *gp23* and *gp25* mutations. Mutant alleles of *gp23* and *gp25* from ICP2 host range mutants were amplified via PCR and cloned into an ampicillin-resistant plasmid, pDL1201 (Fig. S3) by blunt-end ligation (Blunt/TA ligase master mix; New England Biolabs). Mutants with mutations in *gp23* or *gp25* were cloned into separate plasmids. In order to mitigate toxicity in *Escherichia coli* and *V. cholerae*, amplified fragments excluded the start and stop codons of *gp23* and *gp25*, and the intervening gene, *gp24*, was replaced with a kanamycin resistance gene (*neo*). *neo* also separated recombination events occurring within *gp23* and *gp25*. Additionally, the *gp23-neo-gp25* fragment was fused to a LacZα complementing fragment and downstream of a tight arabinose promoter. Recombinant plasmids were first transformed into chemically competent TG1, then moved into *E. coli* SM10(λpir) by electroporation, and finally mated into WT *V. cholerae* or the ΔK139 strain, AC6034. The ΔK139 strain was used to prevent contamination of ICP2 stocks with the K139 temperate phage, which can spontaneously undergo prophage activation.

Plasmid-containing *V. cholerae* strains were grown to early-exponential phase in LB medium supplemented with ampicillin and/or kanamycin (50 or 100 μg/ml), infected with ICP2, and then incubated at 37°C for 4 to 5 h with aeration. During phage multiplication, recombination with the resident plasmid alleles of *gp23* or *gp25* could occur. The high-titer phage stocks from these infections contained both WT and recombinant ICP2.

Host range and EOP assays. Stocks of each phage were serially diluted 10-fold and dribbled across (10 μl) or spotted on (5 μl) soft agarose overlays containing either WT *V. cholerae* or an OmpU mutant strain. The plates were incubated at 37°C overnight, and PFU were counted. Overlays containing *V. cholerae* Δ*ompU* were included as negative controls representing the absence of plaque formation and also served to rule out contamination by other phages used in the lab. The efficiency of plating (EOP) of an ICP2 host range mutant was calculated as the PFU on the OmpU mutant divided by the PFU on WT *V. cholerae*. EOPs below 1 indicate that an ICP2 mutant cannot infect a mutant OmpU strain as well as it can infect the WT. EOPs were averaged from two to five replicate infections. Host range and EOP assays were scanned in order to better visualize small and/or turbid plaques (Epson Scan, version 3.25A).

Phage binding assays. Mid-exponential-phase cultures of WT *V. cholerae* and OmpU receptor mutant strains were washed and resuspended in LB broth. Each strain was diluted to an OD_{600} of 0.1 in 200 μl ($\sim 2 \times 10^7$ CFU) in PCR tubes (catalog no. 1402-4700; USA Scientific). Three replicates of each strain were heat killed at 51°C for 12 min, cooled to 37°C for 2 min in a thermocycler, and then cooled to RT before adsorption. Examination using a phase-contrast microscope showed that the heating process did not lyse the cells. Bacteriophage were added to heat-killed cells at a multiplicity of infection (MOI) of 0.1 ($\sim 2 \times 10^6$ PFU). After the addition of phage and mixing, 90 μl was immediately removed and then serially diluted in LB broth to generate a set of samples representing 0 h of binding. Each dilution series was dribble plated on a soft agarose overlay of WT *V. cholerae*. The remainder of the samples were incubated at RT for 24 h. After incubation, these samples were serially diluted and dribble plated as described above. Plates were incubated at 37°C overnight. Binding efficiency was determined as the ratio of PFU at 24 h to PFU at 0 h.

Before addition to heat-killed cells, phage stocks with titers below 5×10^8 PFU/ml were extracted with 1-octanol to remove lipopolysaccharide (LPS) (37, 38) and preheated for 1 h at 37°C to mitigate discrepancies caused by phage disaggregation at RT. This was not necessary for higher-titer phage stocks that required 1:10 or 1:100 dilution before addition to heat-killed cells. 1-Octanol extraction and preheating did not affect phage predation (Fig. S2).

Phage predation killing assays. In a 96-well plate, 100 μl of washed mid-exponential-phase *V. cholerae* cells diluted to an OD_{600} of 0.2 was infected with 2×10^7 PFU (MOI, 1) in 100 μl of LB broth supplemented with 100 μg/ml of streptomycin (total volume per well, 200 μl). No-phage controls were included to account for growth differences between the host strains. Infections were carried out in technical triplicate, and cultures were incubated at 37°C, with shaking at 205 rpm in a plate reader (BioTek Synergy H1). OD_{600} was

measured every 5 min for 16 h. This assay was conducted twice for phage mutants without a genetic replicate (Fig. S1).

SUPPLEMENTAL MATERIAL

Supplemental material is available online only.

SUPPLEMENTAL FILE 1, PDF file, 2.4 MB.

SUPPLEMENTAL FILE 2, XLSX file, 0.01 MB.

SUPPLEMENTAL FILE 3, XLSX file, 0.02 MB.

ACKNOWLEDGMENTS

This research was supported by National Institutes of Health grants AI055058 (A.C.), AI147658 (A.C.), and GM007310 (A.N.W.L.).

REFERENCES

1. Adhya S, Merril C. 2006. The road to phage therapy. Nature 443:754–755. https://doi.org/10.1038/443754a.
2. Letchumanan V, Chan K-G, Pusparajah P, Saokaew S, Duangjai A, Goh B-H, Ab Mutalib N-S, Lee L-H. 2016. Insights into bacteriophage application in controlling *Vibrio* species. Front Microbiol 7:1114. https://doi.org/10.3389/fmicb.2016.01114.
3. Das B, Verma J, Kumar P, Ghosh A, Ramamurthy T. 2020. Antibiotic resistance in *Vibrio cholerae*: understanding the ecology of resistance genes and mechanisms. Vaccine 38:A83–A92. https://doi.org/10.1016/j.vaccine.2019.06.031.
4. Wittebole X, De Roock S, Opal SM. 2014. A historical overview of bacteriophage therapy as an alternative to antibiotics for the treatment of bacterial pathogens. Virulence 5:226–235. https://doi.org/10.4161/viru.25991.
5. Faruque SM, Naser IB, Islam MJ, Faruque ASG, Ghosh AN, Nair GB, Sack DA, Mekalanos JJ. 2005. Seasonal epidemics of cholera inversely correlate with the prevalence of environmental cholera phages. Proc Natl Acad Sci U S A 102:1702–1707. https://doi.org/10.1073/pnas.0408992102.
6. Faruque SM, Islam MJ, Ahmad QS, Faruque ASG, Sack DA, Nair GB, Mekalanos JJ. 2005. Self-limiting nature of seasonal cholera epidemics: role of host-mediated amplification of phage. Proc Natl Acad Sci U S A 102:6119–6124. https://doi.org/10.1073/pnas.0502069102.
7. Seed KD, Bodi KL, Kropinski AM, Ackermann H-W, Calderwood SB, Qadri F, Camilli A. 2011. Evidence of a dominant lineage of *Vibrio cholerae*-specific lytic bacteriophages shed by cholera patients over a 10-year period in Dhaka, Bangladesh. mBio 2:e00334-10. https://doi.org/10.1128/mBio.00334-10.
8. Seed KD, Yen M, Shapiro BJ, Hilaire IJ, Charles RC, Teng JE, Ivers LC, Boncy J, Harris JB, Camilli A. 2014. Evolutionary consequences of intra-patient phage predation on microbial populations. Elife 3:e03497. https://doi.org/10.7554/eLife.03497.
9. Mathur J, Waldor MK. 2004. The *Vibrio cholerae* ToxR-regulated porin OmpU confers resistance to antimicrobial peptides. Infect Immun 72:3577–3583. https://doi.org/10.1128/IAI.72.6.3577-3583.2004.
10. Sakharwade SC, Mukhopadhaya A. 2015. *Vibrio cholerae* porin OmpU induces LPS tolerance by attenuating TLR-mediated signaling. Mol Immunol 68:312–313. https://doi.org/10.1016/j.molimm.2015.09.021.
11. DiRita VJ, Parsot C, Jander G, Mekalanos JJ. 1991. Regulatory cascade controls virulence in *Vibrio cholerae*. Proc Natl Acad Sci U S A 88:5403–5407. https://doi.org/10.1073/pnas.88.12.5403.
12. Sperandio V, Giron JA, Silveira WD, Kaper JB. 1995. The OmpU outer membrane protein, a potential adherence factor of *Vibrio cholerae*. Infect Immun 63:4433–4438. https://doi.org/10.1128/IAI.63.11.4433-4438.1995.
13. Wibbenmeyer JA, Provenzano D, Landry CF, Klose KE, Delcour AH. 2002. *Vibrio cholerae* OmpU and OmpT porins are differentially affected by bile. Infect Immun 70:121–126. https://doi.org/10.1128/iai.70.1.121-126.2002.
14. Ante VM, Bina XR, Howard MF, Sayeed S, Taylor DL, Bina JE. 2015. *Vibrio cholerae leuO* transcription is positively regulated by ToxR and contributes to bile resistance. J Bacteriol 197:3499–3510. https://doi.org/10.1128/JB.00419-15.
15. Merrell DS, Bailey C, Kaper JB, Camilli A. 2001. The ToxR-mediated organic acid tolerance response of *Vibrio cholerae* requires OmpU. J Bacteriol 183:2746–2754. https://doi.org/10.1128/JB.183.9.2746-2754.2001.
16. Li H, Zhang W, Dong C. 2018. Crystal structure of the outer membrane protein OmpU from *Vibrio cholerae* at 2.2 Å resolution. Acta Crystallogr D Struct Biol 74:21–29. https://doi.org/10.1107/S2059798317017697.
17. Pathania M, Acosta-Gutierrez S, Bhamidimarri SP, Baslé A, Winterhalter M, Ceccarelli M, van den Berg B. 2018. Unusual constriction zones in the major porins OmpU and OmpT from *Vibrio cholerae*. Structure 26:708–721.e4. https://doi.org/10.1016/j.str.2018.03.010.
18. Zhang Y. 2008. I-TASSER server for protein 3D structure prediction. BMC Bioinformatics 9:40. https://doi.org/10.1186/1471-2105-9-40.
19. Roy A, Kucukural A, Zhang Y. 2010. I-TASSER: a unified platform for automated protein structure and function prediction. Nat Protoc 5:725–738. https://doi.org/10.1038/nprot.2010.5.
20. Yang J, Yan R, Roy A, Xu D, Poisson J, Zhang Y. 2015. The I-TASSER suite: protein structure and function prediction. Nat Methods 12:7–8. https://doi.org/10.1038/nmeth.3213.
21. McNair K, Aziz RK, Pusch GD, Overbeek R, Dutilh BE, Edwards R. 2018. Phage genome annotation using the RAST pipeline. Methods Mol Biol 1681:231–238. https://doi.org/10.1007/978-1-4939-7343-9_17.
22. Aziz RK, Bartels D, Best AA, DeJongh M, Disz T, Edwards RA, Formsma K, Gerdes S, Glass EM, Kubal M, Meyer F, Olsen GJ, Olson R, Osterman AL, Overbeek RA, McNeil LK, Paarmann D, Paczian T, Parrello B, Pusch GD, Reich C, Stevens R, Vassieva O, Vonstein V, Wilke A, Zagnitko O. 2008. The RAST server: Rapid Annotations using Subsystems Technology. BMC Genomics 9:75. https://doi.org/10.1186/1471-2164-9-75.
23. Hardies SC, Thomas JA, Black L, Weintraub ST, Hwang CY, Cho BC. 2016. Identification of structural and morphogenesis genes of *Pseudoalteromonas* phage φRIO-1 and placement within the evolutionary history of *Podoviridae*. Virology 489:116–127. https://doi.org/10.1016/j.virol.2015.12.005.
24. Dalia AB, McDonough E, Camilli A. 2014. Multiplex genome editing by natural transformation. Proc Natl Acad Sci U S A 111:8937–8942. https://doi.org/10.1073/pnas.1406478111.
25. De Sordi L, Khanna V, Debarbieux L. 2017. The gut microbiota facilitates drifts in the genetic diversity and infectivity of bacterial viruses. Cell Host Microbe 22:801–808.e3. https://doi.org/10.1016/j.chom.2017.10.010.
26. Rasmussen M, Jacobsson M, Björck L. 2003. Genome-based identification and analysis of collagen-related structural motifs in bacterial and viral proteins. J Biol Chem 278:32313–32316. https://doi.org/10.1074/jbc.M304709200.
27. Engel J, Bächinger HP. 1999. Collagen-like sequences in phages and bacteria. Proc Indian Acad Sci Chem Sci 111:81–86.
28. Mezulis S, Yates CM, Wass MN, Sternberg MJE, Kelley LA. 2019. The Phyre2 web portal for protein modeling, prediction and analysis. Nat Protoc 10:845–858. https://doi.org/10.1038/nprot.2015.053.
29. Granell M, Namura M, Alvira S, Kanamaru S, van Raaij M. 2017. Crystal structure of the carboxy-terminal region of the bacteriophage T4 proximal long tail fiber protein Gp34. Viruses 9:168. https://doi.org/10.3390/v9070168.
30. Dunne M, Denyes JM, Arndt H, Loessner MJ, Leiman PG, Klumpp J. 2018. *Salmonella* phage S16 tail fiber adhesin features a rare polyglycine rich domain for host recognition. Structure 26:1573–1582.e4. https://doi.org/10.1016/j.str.2018.07.017.
31. Trojet SN, Caumont-Sarcos A, Perrody E, Comeau AM, Krisch HM. 2011. The gp38 adhesins of the T4 superfamily: a complex modular determinant of the phage's host specificity. Genome Biol Evol 3:674–686. https://doi.org/10.1093/gbe/evr059.

32. Lee SH, Hava DL, Waldor MK, Camilli A. 1999. Regulation and temporal expression patterns of *Vibrio cholerae* virulence genes during infection. Cell 99:625–634. https://doi.org/10.1016/s0092-8674(00)81551-2.
33. Yen M, Cairns LS, Camilli A. 2017. A cocktail of three virulent bacteriophages prevents *Vibrio cholerae* infection in animal models. Nat Commun 8:14187. https://doi.org/10.1038/ncomms14187.
34. Meibom KL, Blokesch M, Dolganov NA, Wu C-Y, Schoolnik GK. 2005. Chitin induces natural competence in *Vibrio cholerae*. Science 310:1824–1827. https://doi.org/10.1126/science.1120096.
35. Levine MM, Black RE, Clements ML, Cisneros L, Saah A, Nalin DR, Gill DM, Craig JP, Young CR, Ristaino P. 1982. The pathogenicity of nonenterotoxigenic *Vibrio cholerae* serogroup O1 biotype El Tor isolated from sewage water in Brazil. J Infect Dis 145:296–299. https://doi.org/10.1093/infdis/145.3.296.
36. Kamp HD, Patimalla-Dipali B, Lazinski DW, Wallace-Gadsden F, Camilli A. 2013. Gene fitness landscapes of *Vibrio cholerae* at important stages of its life cycle. PLoS Pathog 9:e1003800. https://doi.org/10.1371/journal.ppat.1003800.
37. Bonilla N, Rojas MI, Netto Flores Cruz G, Hung S-H, Rohwer F, Barr JJ. 2016. Phage on tap—a quick and efficient protocol for the preparation of bacteriophage laboratory stocks. PeerJ 4:e2261. https://doi.org/10.7717/peerj.2261.
38. Szermer-Olearnik B, Boratyński J. 2015. Removal of endotoxins from bacteriophage preparations by extraction with organic solvents. PLoS One 10:e0122672. https://doi.org/10.1371/journal.pone.0122672.
39. Sack RB, Miller CE. 1969. Progressive changes of *Vibrio* serotypes in germfree mice infected with *Vibrio cholerae*. J Bacteriol 99:688–695. https://doi.org/10.1128/JB.99.3.688-695.1969.
40. Schild S, Nelson EJ, Camilli A. 2008. Immunization with *Vibrio cholerae* outer membrane vesicles induces protective immunity in mice. Infect Immun 76:4554–4563. https://doi.org/10.1128/IAI.00532-08.
41. Seed KD, Faruque SM, Mekalanos JJ, Calderwood SB, Qadri F, Camilli A. 2012. Phase variable O antigen biosynthetic genes control expression of the major protective antigen and bacteriophage receptor in *Vibrio cholerae* O1. PLoS Pathog 8:e1002917. https://doi.org/10.1371/journal.ppat.1002917.